Pressure dependence of the TO phonon frequency in hcp Zn

2005 J. Phys.: Condens. Matter 17 2121

(http://iopscience.iop.org/0953-8984/17/13/010)

INSTITUTE OF PHYSICS PUBLISHING JOURNAL OF PHYSICS: CONDENSED MATTER

J. Phys.: Condens. Matter **17** (2005) 2121–2128 doi:10.1088/0953-8984/17/13/010

Pressure dependence of the TO phonon frequency in hcp Zn

S L Qiu[1], F Apostol[1] and P M Marcus[2]

[1] Department of Physics, Alloy Research Center, Florida Atlantic University, Boca Raton, FL 33431-0991, USA
[2] IBM Research Division, T J Watson Research Center, Yorktown Heights, NY 10598, USA

Received 24 November 2004, in final form 24 February 2005
Published 18 March 2005
Online at stacks.iop.org/JPhysCM/17/2121

Abstract

Zone-centre transverse optical phonon frequencies $\nu^{TO}(p)$ of hcp Zn as a function of hydrostatic pressure p have been calculated using the full-potential augmented-plane-wave plus local orbitals first-principles method with the generalized gradient approximation and compared with Raman measurements of frequencies under pressure. The oscillatory behaviour of $\nu^{TO}(p)$ found in the pressure range of the anomalies of hcp Zn supports our previous work on Zn, where such effects were shown both in the structural parameters and strongly in the elastic constant $c_{44}(p)$. By integrating the equation of motion using the exact potential and the zero-point and temperature excitations of the Raman active modes we show substantial anharmonic effects which make the frequency of one TO mode the order of 5% below the frequency of the other mode; this split is a large part of the observed line widths.

1. Introduction

The combination of the diamond anvil cell, intense laser light sources and highly sensitive radiation detectors has in recent years made possible Raman line measurements in reflected radiation from a specimen under pressure that provide information about lattice vibration in crystals under high pressure. Crystals with more than one atom in the primitive unit cell, such as hexagonal close-packed (hcp) and diamond structures, have optical-mode vibrations in which atoms in the cell move strongly relative to each other and are Raman active. Such activity depends on variation of the polarizability of the unit cell as the electron distribution changes at the vibration frequency of a particular mode. The frequency of vibration thus modulates the frequency of the incident radiation and produces the sum and difference frequencies of the Raman effect in the reflected radiation. In a one-phonon scattering event in the bulk of the crystal conservation of energy and momentum require that the phonon wavevector be very small, i.e., only zone-centre phonons contribute to the Raman measurement. The symmetry of the hcp structure then restricts Raman activity to the doubly degenerate zone-centre vibration in which alternate hexagonal layers slide on adjacent layers. The energy change in this motion

is the energy of an internal strain. Olijnyk and Jephcoat, in a review of Raman measurements on hcp metals under pressure [1], list a dozen hcp metals in which Raman measurements have been made since 1992.

In a few metals first-principles calculations as a function of pressure of the Raman-active Brillouin zone-centre (Γ point) transverse optical (TO) mode frequency ($\nu^{\mathrm{TO}}(p)$) have been made, including Zn, Mg and Zr. In most cases the calculated frequency follows the experimental values as a function of pressure, but is 5–10% less than experiment and possibly as much as 20% lower when the increase in frequency in going from room temperature measurements to zero temperature values is taken into account.

This paper recalculates the TO mode frequency of hcp Zn as a function of pressure at the Γ point to take advantage of the greater accuracy in determining equilibrium structure under pressure in our paper on anomalies in the structure and elastic properties of hcp Zn under pressure [2]. Here we show that the anomalies are also present in $\nu^{\mathrm{TO}}(p)$. In addition, we show that there is a large anharmonicity in one mode of the doubly degenerate TO vibration, which spreads the TO mode frequencies.

In our paper on anomalies in Zn [2] we have found the equilibrium structure of hcp Zn under pressure p by a first-principles procedure that differs from the usual one, such as [3] and [4] used for hcp Zn. We found equilibrium structural parameters a, c and energies E from the minima of the Gibbs free energy $G = E + pV$ (at 0 K) at p and volume V as a function of structure, i.e., of a and c, whereas the usual procedure [3, 4] finds equilibrium from minima of $E(c/a)$ at constant V. From the minima of E at several V, the pressure p is then obtained by differentiating $E_{\min}(V)$ with respect to V.

We give reasons in [2] why we believe our equilibrium structures are more accurate than those found by the usual procedure. Not only do we find structural anomalies in Zn and Cd that agree well with experiment, but we also calculate elastic quantities like $c_{44}(p)$ which show strong oscillations in the pressure range of the anomalies.

Here we make a further test of our accuracy by using the equilibrium state at each p to calculate the zone-centre transverse optical mode frequency $\nu^{\mathrm{TO}}(p)$ of hcp Zn. This frequency has been measured optically at pressures in the anomalous range of p as a Raman line [5]. Contrary to the previous discussion of theory and experiment in [5], we find definite oscillations in $\nu^{\mathrm{TO}}(p)$ in the pressure range of the anomalies. In addition we use our values of $c_{44}(p)$ to make a quantitative test of an empirical formula relating ν^{TO} and c_{44} [5, 6] and show that it is rather poor for hcp Zn.

We also study the anharmonic content of the Raman-active mode by integrating the equation of motion of the transverse optic mode in the exact potential controlling the motion. The potential contains all anharmonic contributions, which are shown to be large (at 300 K) for one direction of vibration and negligible for the orthogonal direction. The split in the two frequencies due to the anharmonic part of the potential is shown to be a substantial part of the observed line widths as functions of p.

The procedures are described in section 2, the results are given in section 3 and discussion of the results in section 4.

2. Procedures

First-principles calculations on hcp Zn under hydrostatic pressure were performed using the full-potential augmented-plane-wave plus local orbitals (APW + lo) method together with the Perdew–Burke–Ernzerhof generalized-gradient-approximation (PBE-GGA) as implemented in the WIEN2k package [7]. The APW + lo method expands the Kohn–Sham orbitals in atomic-like orbitals inside the atomic spheres and plane waves in the interstitial region. A

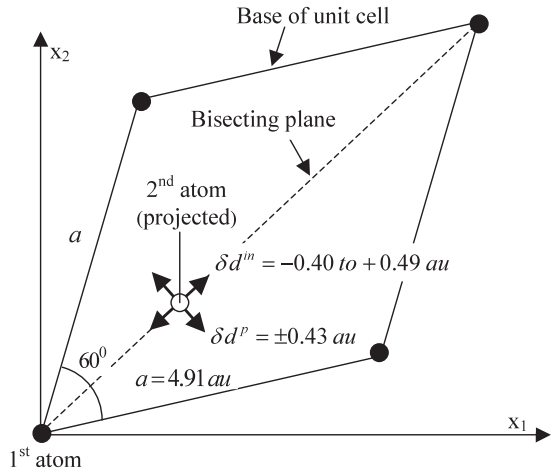

Figure 1. The base of an hcp unit cell with $\gamma = 60°$ rotated 15° about the c (or x_3) axis so that the basal rhombus is oriented symmetrically with respect to the orthogonal axes x_1 and x_2. The equilibrium position of the second atom in the unit cell is projected on the base.

plane-wave cutoff $R_{\mathrm{MT}}K_{\max} = 7$, $R_{\mathrm{MT}} = 1.6$ au, $G_{\max} = 14$ and mixer $= 0.05$ were used in all the calculations; 5300 k-points in the irreducible Brillouin zone were used in the calculations of the Gibbs free energy along the epitaxial Bain path (G^{EBP}) and in the calculation of the elastic constants. The k-space integration was done by the modified tetrahedron method. Tests with larger basis sets and different Brillouin zone samplings yielded only very small changes in the results. The convergence criterion on the energies is set at 1×10^{-3} mRyd (10^{-6} Ryd) per atom.

The procedures for calculating the pressure dependence of $\nu^{\mathrm{TO}}(p)$ are as follows.

(1) Calculate G^{EBP} to find the equilibrium lattice parameters and elastic constants as functions of pressure. The details of the procedure for finding the equilibrium states and the elastic constants of the hcp lattice are given in our previous reports [2, 8–11]. Briefly, the equilibrium state is found from the thermodynamic result that at a given pressure p the Gibbs free energy (at zero temperature) $G \equiv E(a, c) + pV(a, c)$ is a minimum with respect to both the hcp structure parameters a and c, where E is the energy/atom and V the volume/atom. The double minimum is conveniently found from a minimum of G^{EBP}, where the EBP is adapted to finite pressure. The elastic constants are then found as second strain derivatives of G in the equilibrium state at p, while p remains constant. This procedure finds the structural parameters and elastic constants directly as functions of p.

(2) Calculate the vibrational potential δE versus displacements δd of the second atom in the unit cell from the equilibrium structure at given pressures. Figure 1 shows the projected hcp unit cell used for δE versus δd calculations (the three-dimensional unit cell is given in our previous report [8]). In a conventional two-atom hcp unit cell $\alpha = \beta = 90°$, $\gamma = 120°$, $a = b$ and the two atoms are located at (0, 0, 0) and (2/3, 1/3, 1/2) respectively with vector components along and in units of the lengths of the lattice vectors ($\vec{a}, \vec{b}, \vec{c}$).

To calculate δE versus δd it is more convenient to use an unconventional two-atom hcp unit cell with $\gamma = 60°$ and to rotate the unit cell by 15° about the c (x_3) axis, so as to have the basal rhombus symmetrically oriented with respect to the orthogonal axes x_1 and x_2, as shown in figure 1. This orientation makes the internal relaxation (for the relaxed elastic constant calculation) one dimensional for strains that preserve the reflection symmetry of the bisecting

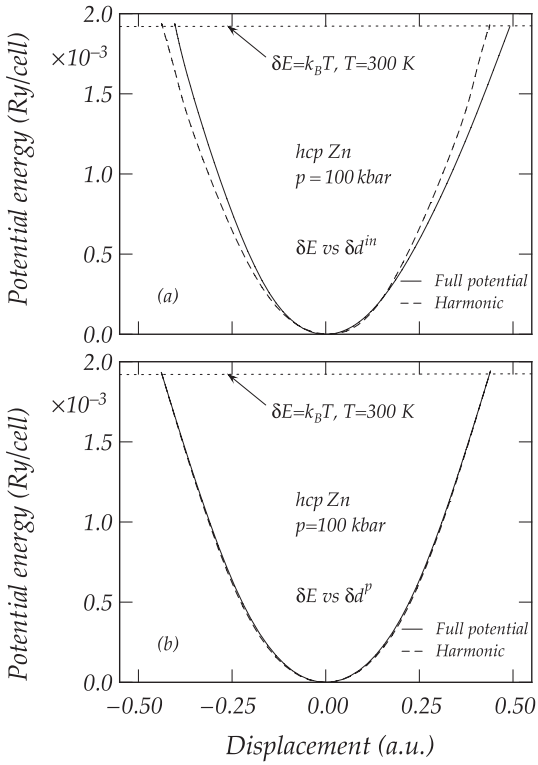

Figure 2. (a) δE versus δd^{in} and (b) δE versus δd^{p} curves at $p = 100$ kbar. The solid curves denote the full potential, the dashed curves denote the harmonic part of the potential and the horizontal dotted lines correspond to $\delta E = k_{\mathrm{B}}T$ with $T = 300$ K at $p = 100$ kbar.

plane. (Note that the elastic constants are independent of the orientation of the x_1 and x_2 axes due to sixfold symmetry.) Then the position of the second atom in the equilibrium state is (1/3, 1/3, 1/2). Two directions of δd designated δd^{in} and δd^{p} are considered, as shown in figure 1, and both of them are in atomic units. The position of the second atom with δd^{in} is $\left(\frac{1}{3} + \frac{\delta d^{\mathrm{in}}}{\sqrt{3}a}, \frac{1}{3} + \frac{\delta d^{\mathrm{in}}}{\sqrt{3}a}, \frac{1}{2}\right)$ while with δd^{p} the position is $\left(\frac{1}{3} + \frac{\delta d^{\mathrm{p}}}{a}, \frac{1}{3} - \frac{\delta d^{\mathrm{p}}}{a}, \frac{1}{2}\right)$. Both δd^{in} and δd^{p} are perpendicular to the c-axis corresponding to the displacements in the TO mode. The value of $a = 4.91$ au shown in figure 1 is the equilibrium lattice parameter of the base of the unit cell at $p = 100$ kbar obtained from the G^{EBP} calculations. The values of δd^{in} and δd^{p} shown in figure 1 are the magnitudes of the vibrations corresponding to $\delta E = k_{\mathrm{B}}T$ with $T = 300$ K at $p = 100$ kbar.

Figures 2(a) and (b) show δE versus δd^{in} and δE versus δd^{p} curves respectively at $p = 100$ kbar. The solid curves represent the full potential, the dashed curves represent the harmonic part of the potential and the horizontal dotted lines correspond to $\delta E = k_{\mathrm{B}}T$ with $T = 300$ K at $p = 100$ kbar. Such calculations are repeated at different pressures from 0 to 200 kbar in order to obtain the pressure dependence of $\nu^{\mathrm{TO}}(p)$.

(3) Calculate $\nu^{\mathrm{TO}}(p)$ from the full δE versus δd curves by integration over the full potential (Simpson's rule with 999 points). For convenience in writing equations let E and x represent δE and δd respectively. The equation of motion of the vibration is

$$\ddot{x} = -\frac{1}{m}\frac{\partial E}{\partial x}, \tag{1}$$

where $m = M_{\mathrm{Zn}}/2$ is the reduced mass of the atom and M_{Zn} is the atomic mass of Zn. Equation (1) can be integrated and the solution over the full orbit gives the period of the vibration as

$$T = 2\int_{x_{\max 1}}^{x_{\max 2}} \frac{\mathrm{d}x}{\left[\frac{2}{m}(E(x_{\max}) - E(x))\right]^{1/2}}, \tag{2}$$

where $E(x_{\max}) = E(x_{\max 1}) = E(x_{\max 2}) = k_{\mathrm{B}}T$ with $T = 300$ K, and $x_{\max 1}$ is negative while $x_{\max 2}$ is positive.

The integral is singular but integrable: expand the function $E(x)$ around $x_{\max}$ (which represents either $x_{\max 1}$ or $x_{\max 2}$),

$$E(x) = E(x_{\max}) + A(x - x_{\max}) + f(x), \tag{3}$$

where $|x| < |x_{\max}|$ and $f(x)$ has higher powers of $(x - x_{\max})$. Then the singularity can be subtracted out and integrated analytically:

$$\int_x^{x_{\max}} \frac{\mathrm{d}x}{[E(x_{\max}) - E(x)]^{1/2}} = \int_x^{x_{\max}} g(x)\,\mathrm{d}x + 2\left(\frac{x_{\max} - x}{A}\right)^{\frac{1}{2}}, \tag{4}$$

where

$$g(x) \equiv \frac{1}{[E(x_{\max}) - E(x)]^{1/2}} - \frac{1}{[A(x_{\max} - x)]^{1/2}}, \tag{5}$$

and $g(x)$ can be integrated numerically. This procedure is used just for small intervals near $x_{\max}$.

(4) Calculate $\nu^{\mathrm{TO}}(p)$ from c_{44} using the empirical relation (6) given in [5, 6].

$$\nu^{\mathrm{TO}} = \frac{1}{\pi}\sqrt{\frac{\sqrt{3}a^2c_{44}}{Mc}}. \tag{6}$$

In (6) a and c are the lattice constants, and M is the atomic mass. The elastic constant c_{44} of hcp Zn as a function of pressure has been calculated using the procedures given in our previous reports [2, 9]. The relation (6) can then be tested quantitatively for hcp Zn.

3. Results

Figures 3 shows the zone-centre TO mode frequency $\nu^{\mathrm{TO}}(p)$ as a function of pressure. The open diamonds in figures 3(a) and (b) are the experimental data measured by Raman spectroscopy at room temperature from [5]. The open circles in figures 3(a) and (b) are the calculated frequency–pressure data at zero temperature found in a previous calculation using the 'frozen-phonon' method, also from [5]. The solid circles and solid squares in figures 3(a) are calculated from the numerical integration of the δE versus δd^{in} curves of the full and harmonic potentials respectively. The solid triangles in figures 3(a) are obtained from the integration of the δE versus δd^{p} curves. For the vibration perpendicular to the bisecting plane both the full and harmonic potentials give the same frequency at each given pressure up to δE at 300 K.

Figure 4 demonstrates the oscillatory behaviour of $\nu^{\mathrm{TO}}(p)$ in the pressure range of the anomalies of hcp Zn. All the data (except the δd^{in} harmonic data) shown in figure 3 are re-plotted in figure 4 with expanded scales along with the data (open triangles) calculated from the relaxed c_{44} using (6). Measurement of $\nu^{\mathrm{TO}}(p)$ for Cd would be particularly interesting because the anomalies in Cd are greater than in Zn [2].

The open circles in figure 5 are the experimental line widths of the Raman spectra of the TO mode of hcp Zn as a function of pressure [5]. The solid dels denote the frequency difference between the solid circles and the solid squares in figure 3(a), which are calculated from the δE versus δd^{in} curves of the full and harmonic potentials respectively.

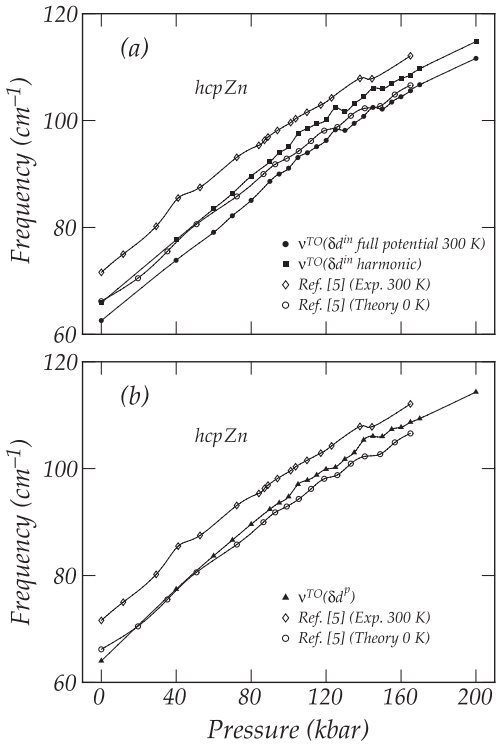

Figure 3. Zone-centre TO mode frequency as a function of pressure. The open diamonds and open circles in (a) and (b) are the experimental and theoretical data from [5]. The solid circles and solid squares in (a) are calculated from the δE versus δd^{in} curves of the full and harmonic potentials respectively. The solid triangles in (b) are obtained from the δE versus δd^{p} curves. In both (a) and (b) the solid curves interpolate between the data points.

4. Discussion

The oscillation in $\nu^{\mathrm{TO}}(p)$ shown in figures 3 and 4 supports our belief that our procedure for finding equilibrium at a given p is more accurate than the usual procedure based on minima of $E(c/a)$ at constant V. The previous theoretical result in [5] was interpreted as a smooth curve in figure 2 of [5], although some irregularity is shown in figure 3 of [5]. Here we show clearly visible oscillations of ν^{TO} at 145, 125, 105 and 95 kbar which are present in both the full potential and harmonic part of the potential for the in-plane displacement δd^{in}. Somewhat different oscillations appear at 140, 120 and 110 kbar for the out-of-plane displacement δd^{p}, which is entirely harmonic. The experimental data show some anomalies at 140 kbar, and possibly at 110 and 95 kbar. Comparison with the original data, which are not tabulated in [5], might verify the possible anomalies which are suggested by the theoretical results.

The full potential shown in figure 2(a) for the in-plane displacement δd^{in} shows a substantial asymmetry, which is due to dependence of the full potential on $(\delta d^{\mathrm{in}})^3$ terms in the expansion around equilibrium. Such terms are forbidden in the potential for δd^{p} in figure 2(b) since the plane bisecting the 60° vertex angle in figure 1 is a plane of reflection symmetry for δd^{p}; the fourth-order terms in δd^{p} are negligible at $\delta E = 2$ mRyd corresponding to the phonon energy at 300 K.

The comparison of calculated $\nu^{\mathrm{TO}}(p)$ with values calculated with the empirical formula (6) using calculated $c_{44}(p)$ values in figure 4 shows poor correspondence. The formula (6) values

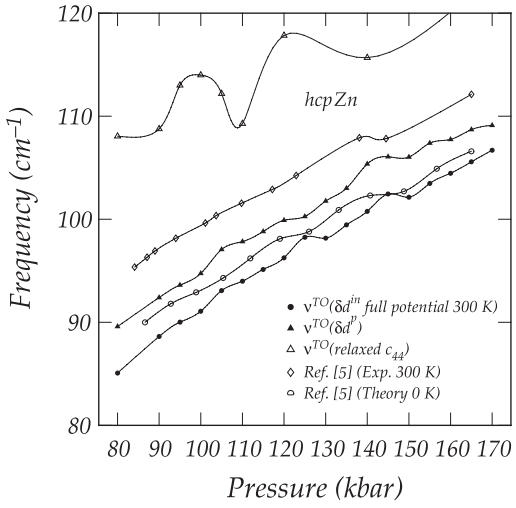

Figure 4. Oscillatory behaviour of the TO mode frequencies in the pressure range of the anomalies of hcp Zn. The open triangles are calculated from the relaxed c_{44} using (6). All other data are the same as in figure 3 but with a smaller pressure range. The solid curves interpolate between the data points.

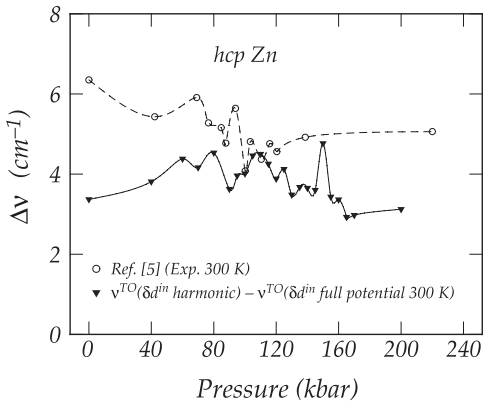

Figure 5. The open circles are the experimental line widths of the Raman spectra versus pressure from [5]. The solid dels are the frequency differences between ν^{TO} (δd^{in} *harmonic*) and ν^{TO} (δd^{in} *full potential* 300 K) as a function of pressure. The solid and dashed curves interpolate between the data points.

are high by ∼30% and the anomalous oscillations are much stronger than in the first-principles $\nu^{\mathrm{TO}}(p)$. The comparison uses relaxed values of c_{44}; use of unrelaxed values, which are larger, would increase the discrepancy.

The anharmonic content of $E(\delta d^{\mathrm{in}})$, which lowers the full-potential frequencies by ∼5%, produces a spread of frequencies from ν^{TO} obtained with δd^{p} to ν^{TO} obtained with δd^{in}. The spread of frequencies is shown in figure 5 to be a substantial part of the observed line widths plotted in figure 5. The downward trend of the calculated frequency spread from 60 to 140 kbar also seems to correspond to the experimental line-width values.

Acknowledgments

The calculations were carried out using the computational resources BOCA4 Beowulf at Charles E Schmidt College of Science, Florida Atlantic University. P M Marcus thanks IBM for providing facilities as an Emeritus member of the Thomas J Watson Research Center.

References

[1] Olijnyk H and Jephcoat A P 2002 *Metall. Mater. Trans.* A **33** 743
[2] Qiu S L, Apostol F and Marcus P M 2004 *J. Phys.: Condens. Matter* **16** 6405
[3] Neumann G-S, Stixrude L and Cohen R E 2001 *Phys. Rev.* B **63** 054103
[4] Novikov D L, Freeman A J, Christensen N E, Svane A and Rodriguez C O 1997 *Phys. Rev.* B **56** 7206
[5] Olijnyk H, Jephcoat A P, Novikov D L and Christensen N E 2000 *Phys. Rev.* **62** 5508
[6] Olijnyk H and Jephcoat A P 2002 *High Pressure Res.* **22** 43
[7] Blaha P, Schwarz K, Madsen Kvasnicka G D and Luitz J 2001 *WIEN2k, An augmented Plane Wave + Local Orbitals Program for calculating Crystal Properties* (Karlheinz Schwarz, Technical Universität Wien, Austria) ISBN 3-9501031-1-2
Blaha P, Schwarz K and Sorantin P 1990 *Comput. Phys. Commun.* **59** 399
[8] Qiu S L and Marcus P M 2003 *Phys. Rev.* B **68** 054103
[9] Qiu S L and Marcus P M 2003 *J. Phys.: Condens. Matter* **15** L755
[10] Marcus P M, Ma H and Qiu S L 2002 *J. Phys.: Condens. Matter* **14** L525
[11] Marcus P M and Qiu S L 2004 *J. Phys.: Condens. Matter* **16** 8787